

Anti-apoptotic Effects of Human Wharton's Jelly-derived Mesenchymal Stem Cells on Skeletal Muscle Cells Mediated via Secretion of XCL1

Soojin Kwon^{1,2}, Soo Mi Ki², Sang Eon Park¹⁻⁴, Min-Jeong Kim¹, Brian Hyung⁵, Na Kyung Lee¹⁻⁴, Sangmi Shim⁶, Byung-Ok Choi^{2,3}, Duk L Na^{3,4}, Ji Eun Lee^{2,7} and Jong Wook Chang^{1,2}

¹Stem Cell & Regenerative Medicine Institute, Samsung Medical Center, Seoul, Republic of Korea; ²Department of Health Sciences and Technology, SAIHST, Sungkyunkwan University, Seoul, Republic of Korea; ³Department of Neurology, Samsung Medical Center, Sungkyunkwan University School of Medicine, Seoul, Republic of Korea; ⁴Neuroscience Center, Samsung Medical Center, Seoul, Republic of Korea; ⁵McGill University, Montreal, Quebec, Canada; ⁶Department of Biomedical Sciences, College of Medicine, Seoul National University, Seoul, Republic of Korea; ⁷Samsung Genome Institute, Samsung Medical Center, Seoul, Republic of Korea

The role of Wharton's jelly-derived human mesenchymal stem cells (WJ-MSCs) in inhibiting muscle cell death has been elucidated in this study. Apoptosis induced by serum deprivation in mouse skeletal myoblast cell lines (C2C12) was significantly reduced when the cell lines were cocultured with WJ-MSCs. Antibody arrays indicated high levels of chemokine (C motif) ligand (XCL1) secretion by cocultured WJ-MSCs and XCL1 protein treatment resulted in complete inhibition of apoptosis in serum-starved C2C12 cells. Apoptosis of C2C12 cells and loss of differentiated C2C12 myotubes induced by lovastatin, another muscle cell death inducer, was also inhibited by XCL1 treatment. However, XCL1 treatment did not inhibit apoptosis of cell lines other than C2C12. When XCL1-siRNA pretreated WJ-MSCs were cocultured with serum-starved C2C12 cells, apoptosis was not inhibited, thus confirming that XCL1 is a key factor in preventing C2C12 cell apoptosis. We demonstrated the therapeutic effect of XCL1 on the zebrafish myopathy model, generated by knock down of a causative gene *ADSSL1*. Furthermore, the treatment of XCL1 resulted in significant recovery of the zebrafish skeletal muscle defects. These results suggest that human WJ-MSCs and XCL1 protein may act as promising and novel therapeutic agents for treatment of myopathies and other skeletal muscle diseases.

Received 8 January 2016; accepted 16 June 2016; advance online publication 19 July 2016. doi:10.1038/mt.2016.125

INTRODUCTION

Apoptosis plays a pivotal role in tissue homeostasis and its dysregulation has been implicated in the fundamental pathogenesis of many diseases.^{1,2} The diverse roles played by apoptosis in

regulating various physiological and pathological functions suggest its importance as a significant target for development of novel medical treatments for existing incurable diseases.^{3,4}

Recently, significant reports have demonstrated that sarcomeric muscles (skeletal muscle fibers and cardiomyocytes) are prone to apoptosis.⁵ In many degenerative muscle diseases, myoblast and muscle fibers die due to atrophy, exercise-induced muscle damage, aging, dystrophinopathy, and myopathies with inflammation and mitochondrial defects.⁶⁻⁸ Most of the diseased muscle tissues show both elevated TUNEL-positive myonuclei and expression of apoptotic proteins during disease progression. Therefore, decreasing the rate of abnormal apoptosis progression may be a therapeutic approach to preserve muscle function.^{9,10}

Currently, treatment strategies for muscular diseases are limited, while there exists no specific treatment for certain diseases. Nevertheless, as muscle wasting is the prime outcome of muscular diseases, preventing muscle cell death is one of the approaches for a strategic treatment.¹¹⁻¹³

Recently numerous clinical trials have shown that naive human mesenchymal stem cells (MSCs) are safe and beneficial to be considered for design of treatment methods for various pathologies.¹⁴⁻¹⁶ The primary mechanism of their therapeutic effects is via secretion of paracrine factors under abnormal and diseased cellular environments. For example, the paracrine action of human MSC has been demonstrated to prevent cell death and induce proliferation of endogenous progenitor cells.¹⁷⁻²¹ Therefore, human MSCs have been described as injury drug store.^{22,23}

Lately, numerous paracrine factors have been identified through proteomic approaches. Studies have shown that these recombinant protein treatments exhibit identical therapeutic effects as human MSCs, both *in vitro* and *in vivo*. Further investigations on human MSC paracrine factors are required to gain complete understanding about the underlying therapeutic

The first two authors contributed equally to this work.

Correspondence: Jong Wook Chang, Stem Cell & Regenerative Medicine Institute, Samsung Medical Center, 06351, Seoul, Republic of Korea; Department of Health Sciences and Technology, Samsung Advanced Institute for Health Sciences and Technology (SAIHST), Sungkyunkwan University, 06351, Seoul, Republic of Korea. E-mail: jongwook.chang@samsung.com/Changjw@skku.edu or Ji Eun Lee, Department of Health Sciences and Technology, Samsung Advanced Institute for Health Sciences and Technology (SAIHST), Sungkyunkwan University, 06351, Seoul, Republic of Korea. E-mail: jieun.lee@skku.edu

mechanisms of MSCs and develop novel treatment strategies employing recombinant proteins.^{17–19}

In this study, we investigated whether human Wharton's jelly-derived MSCs (WJ-MSCs) could rescue both *in vitro* and *in vivo* models of skeletal muscle from cell death via paracrine activity. Furthermore, we identified chemokine (C motif) ligand (XCL1) as the key WJ-MSCs derived paracrine factor that mediates anti-apoptotic effect.

RESULTS

Coculture with human WJ-MSCs reduced serum-starvation-induced C2C12 cell death

The effects of WJ-MSCs on serum-deprived C2C12 cell death were evaluated through coculture. Mouse skeletal myoblast, C2C12 cells, were cultured in serum-deprived media to induce apoptosis. Images taken at 12 and 24 hours of serum-starvation exhibited typical patterns of apoptosis. The extent of apoptotic floating C2C12 cells was significantly decreased upon coculturing with WJ-MSC (Supplementary Figure S1). The obtained results were confirmed through fluorescence-activated cell-sorting (FACS) analysis using annexin V/7-AAD staining (Figure 1a,b) and Western blot analysis of poly ADP-ribose polymerase (PARP) cleavages (Figure 1c,d). A marked reduction in annexin V and 7-AAD staining was observed in serum-deprived C2C12 cells cocultured with WJ-MSCs. Furthermore, a significant reduction in PARP fragments in serum-deprived C2C12 cells cocultured with WJ-MSCs was observed, as compared with C2C12 cell cultured alone. Human WJ-MSCs prepared as described in the Materials and Methods section were characterized according to the MSC criteria set by International Society for Cell Therapy (Supplementary Figure S2).²⁴ These results confirmed that WJ-MSCs were the primary factor in preventing C2C12 cell death. However, as the two cell types were physically separated by the transwell insert, the mechanism behind the observed effect on serum-starved C2C12 cells involved release of soluble factors by WJ-MSCs.

Identification of secreted proteins from WJ-MSC including anti-apoptotic XCL1

The conditioned media of each sample group were analyzed by three-independent antibody arrays to identify the soluble factors secreted by WJ-MSCs cocultured with C2C12 cells (Figure 2a). The XCL1, IL-3R, and Smad5 were consistently elevated in cocultured media, as compared to that of WJ-MSCs alone (Figure 2b). Results from XCL1 quantification in conditioned media of MSC cultures are shown in Figure 2c. The concentration of secreted XCL1 in each conditioned media was measured by human XCL1-ELISA. When cultured WJ-MSC alone, the concentration of the secreted XCL1 proteins was 4.17 ± 0.32 ng/ml and when cocultured with C2C12 cells, the concentration increased to 7.34 ± 0.57 ng/ml (Figure 2c). Therefore, out of the three, XCL1 was selected as the only secretory protein for further experimentation. *In vitro* serum-starved C2C12 cells were treated with recombinant XCL1 proteins in a dose-dependent manner. FACS analysis and PARP cleavage assay demonstrated treatment range of 5, 10, 20, and 50 ng/ml of XCL1 as effective range in reducing cell apoptosis (Figure 3). Also, FACS analysis illustrated enhancement in the number of viable cells upon treatment with XCL1 in a dose-dependent

manner (Figure 3a,b). PARP cleavage was blocked in C2C12 cells treated with XCL1 as per Western blot analyses (Figure 3c,d). Furthermore, C2C12 cells treated with 8 ng/ml of XCL1, which was the equivalent physiological concentration of XCL1 proteins secreted through the coculture system (Figure 2c), showed similar anti-apoptotic effects in a time-dependent manner (Figure 3e,f). XCL1 exerted a stronger inhibitory effect on myoblast apoptosis, as compared to pan-caspase inhibitor, which is commonly employed as a potent apoptosis inhibitor (Figure 3g,h). These data suggested WJ-MSC-derived XCL1 as a potential anti-apoptotic paracrine factor and the concentration of XCL1 recombinant protein equivalent to the physiological concentration of XCL1 as effective concentration in inducing anti-apoptotic effects.

Absence of anti-apoptotic effect of XCL1 in other cell types

Based on the property of XCL1 to rescue C2C12 cells from cell death, we further tested the anti-apoptotic effects of XCL1 on other cell types like: HT22 (mouse hippocampal neurons), NIH3T3 cell (mouse fibroblast), BEAS-2B (human lung epithelial cells), and IMCD3 cells (mouse kidney duct cells). Amyloid- β 42 and the proteasome inhibitor MG132, which are well-known apoptosis inducers in the Alzheimer's disease model, were used to induce cell death in HT22 cell^{25,26}; the HT22 cells were treated with amyloid- β 42 (1 μ mol/l) or MG132 (5 μ mol/l) for 24–48 hours for induction of apoptosis. FACS analysis and PARP cleavage assay showed that subsequent XCL1 treatment failed to rescue the neuronal cells from apoptosis (Figure 4a,b). Apoptosis in S16 rat Schwann cells induced by the endoplasmic reticulum stress inducer, thapsigargin (1 μ mol/l) for 12 hours, was also not inhibited by XCL1 treatment (Figure 4c,d). Furthermore, XCL1 treatment failed to inhibit apoptosis in MG132-exposed NIH3T3 cell (mouse fibroblast), BEAS-2B (human lung epithelial cells), and IMCD3 cells (mouse kidney duct cells) (Supplementary Figure S3).

Previous studies have reported that the treatment of Lovastatin, an inhibitor of cholesterol synthesis, leads to skeletal muscle atrophy.²⁷ We therefore used Lovastatin as another apoptosis-inducing agent to determine whether XCL1 generally inhibits C2C12 cell death. We treated both, C2C12 myoblasts and 7-day differentiated C2C12 myotubes with various concentrations of Lovastatin. As compared with control-C2C12 myoblasts treated with an equal volume of the vehicle, Lovastatin-induced PARP cleavage was completely blocked in C2C12 myoblast by XCL1 treatment (Figure 5a,b). In addition, recombinant XCL1 treatment reduced loss of myotubes induced by lovastatin exposure (Figure 5c,d), which was quantified by measuring the expression of myosin heavy chain (MHC) (Figure 5d). These results suggested that the anti-apoptotic effects of XCL1 might be more favorable for skeletal muscle cells than for other types of cells including SH-SY5Y, S16, NIH3T3, BEAS-2B, and IMCD3 (mouse kidney duct cells, Inner Medullary Collecting Duct 3) cells.

XCL1 is required for the anti-apoptotic effect of human WJ-MSC

XCL1 small-interfering RNA (siRNA) was used to confirm whether XCL1 secretion was the primary mechanism responsible for the anti-apoptotic effect of WJ-MSCs on C2C12 cells.

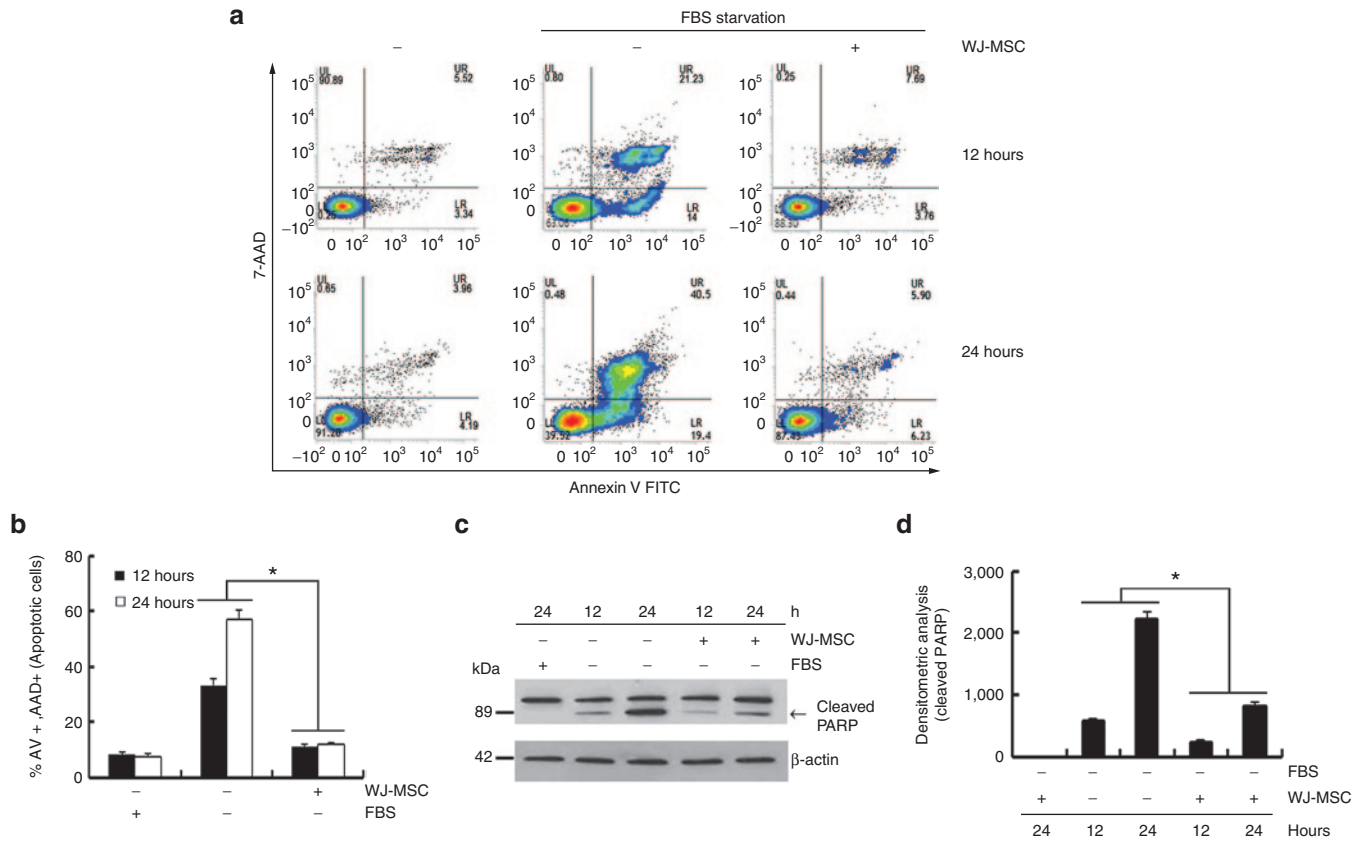


Figure 1 Coculturing with human Wharton’s jelly-derived human mesenchymal stem cells (WJ-MSCs) reduced serum starvation-induced C2C12 cell death via secretion of soluble factors. C2C12 cells were serum-deprived during culture both in the absence and presence of human WJ-MSC (1×10^5 cells/well) for 12 and 24 hours in a transwell chamber. C2C12 cells alone and C2C12 cells cocultured with human WJ-MSC in the absence of serum were analyzed by fluorescence-activated cell-sorting (FACS) analysis of cells stained with annexin V/7-AAD (**a,b**) or Western blot analysis with anti-poly ADP-ribose polymerase (PARP) antibody (**c,d**). The arrow indicates cleaved PARP during apoptosis. (**b**) Percentage of apoptotic cells by FACS analysis ($*P < 0.05$, $n = 3$). (**d**) The cleaved PARP bands were analyzed through densitometry ($*P < 0.05$, $n = 3$)

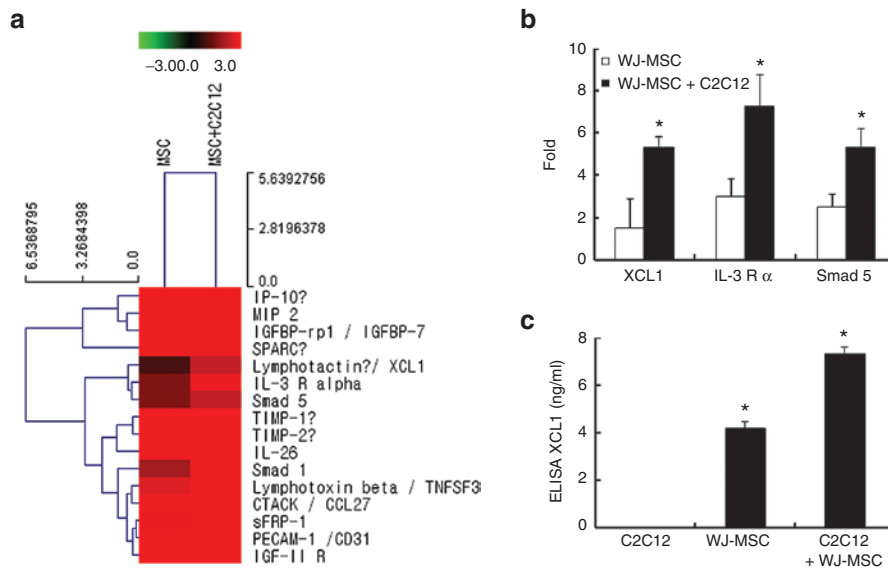


Figure 2 Identification of XCL1 as a paracrine factor of Wharton’s jelly-derived human mesenchymal stem cell (WJ-MSC) during coculture. Secreted proteins in the media collected from the experiments were measured using the RayBio Biotin Label-based Human Antibody. (**a,b**) Increased fold of spot intensity of XCL1, IL-3 R, and smad5 in cocultured cells as compared to WJ-MSC alone. (**c**) The conditioned media was collected from C2C12, WJ-MSC alone, and cocultured cells. Concentration of secreted XCL1 in each conditioned media was measured by XCL1 ELISA kit ($*P < 0.05$, $n = 3$).

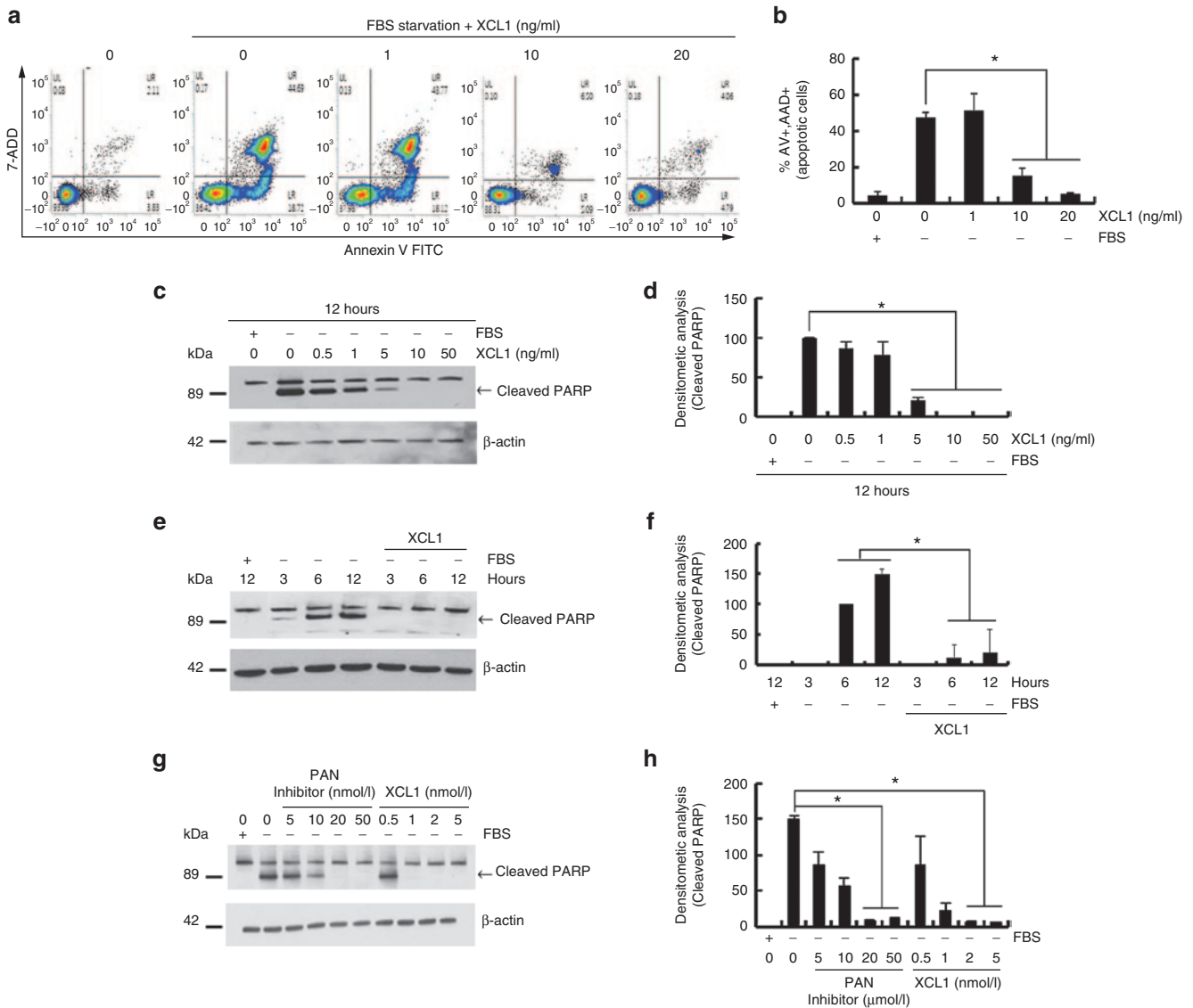


Figure 3 Recombinant XCL1 protein inhibited serum starvation-induced apoptosis of C2C12 cells. C2C12 cell was serum-deprived during culture both in the absence or presence of recombinant XCL1 proteins (1, 10, and 20 ng/ml) for 12 hours. **(a)** Fluorescence-activated cell-sorting (FACS) analysis of cells stained with annexin V/7-AAD. **(b)** Percentage of apoptotic cells by FACS analysis ($*P < 0.05$, $n = 3$). **(c)** Harvested cells were analyzed by Western blot analysis with anti-poly ADP-ribose polymerase (PARP) antibody. **(d)** PARP cleaved bands were analyzed by densitometry ($*P < 0.05$, $n = 3$). **(e)** Serum-deprived C2C12 cells were treated with recombinant XCL1 (8 ng/ml) in a time-dependent manner. **(f)** PARP cleavage was monitored by Western blot analysis ($*P < 0.05$, $n = 3$). **(g)** Serum-deprived C2C12 cells were treated with either PAN caspase inhibitor (z-VAD-FMK) or XCL1 protein in a dose-dependent manner for 24 hours. **(h)** Apoptotic cells were analyzed by Western blot with anti-PARP antibody. ($*P < 0.05$, $n = 3$).

Similar to our previous data, a reduction in apoptosis and PARP cleavage of C2C12 cells were observed following WJ-MSC coculture (Figure 6a,b). To monitor the loss of XCL1 function depending on particular siRNA treatment, one group of WJ-MSCs was pretreated with XCL1-siRNA1 and another with XCL1-siRNA2 for 24 hours. When these WJ-MSC groups were cocultured with serum-starved C2C12 cells, no anti-apoptotic effects were observed in either groups (Figure 6a,b). Remarkably, addition of recombinant XCL1 protein restored anti-apoptotic effects in both XCL1 siRNA treated cocultures (Figure 6a,b). Western blot analysis employing anti-PARP antibody was used to monitor PARP cleavage at each condition (Figure 6b). In addition, we measured the concentration

of secreted XCL1 from the siRNA experiment to confirm the specificity of each siRNA for XCL1. After treatment of XCL1 siRNA, secretion of XCL1 was completely reduced in the conditioned media of cocultured cells as compared to that collected from WJ-MSCs treated with control siRNA (Figure 6c). These results indicated that WJ-MSCs protect C2C12 cells from serum deprivation-induced cell death primarily via secretion of XCL1 protein.

Human XCL1 inhibits apoptosis in zebrafish skeletal muscle

The zebrafish model system was employed to verify muscle-specific role of XCL1 *in vivo*. We had recently identified *ADSSL1*

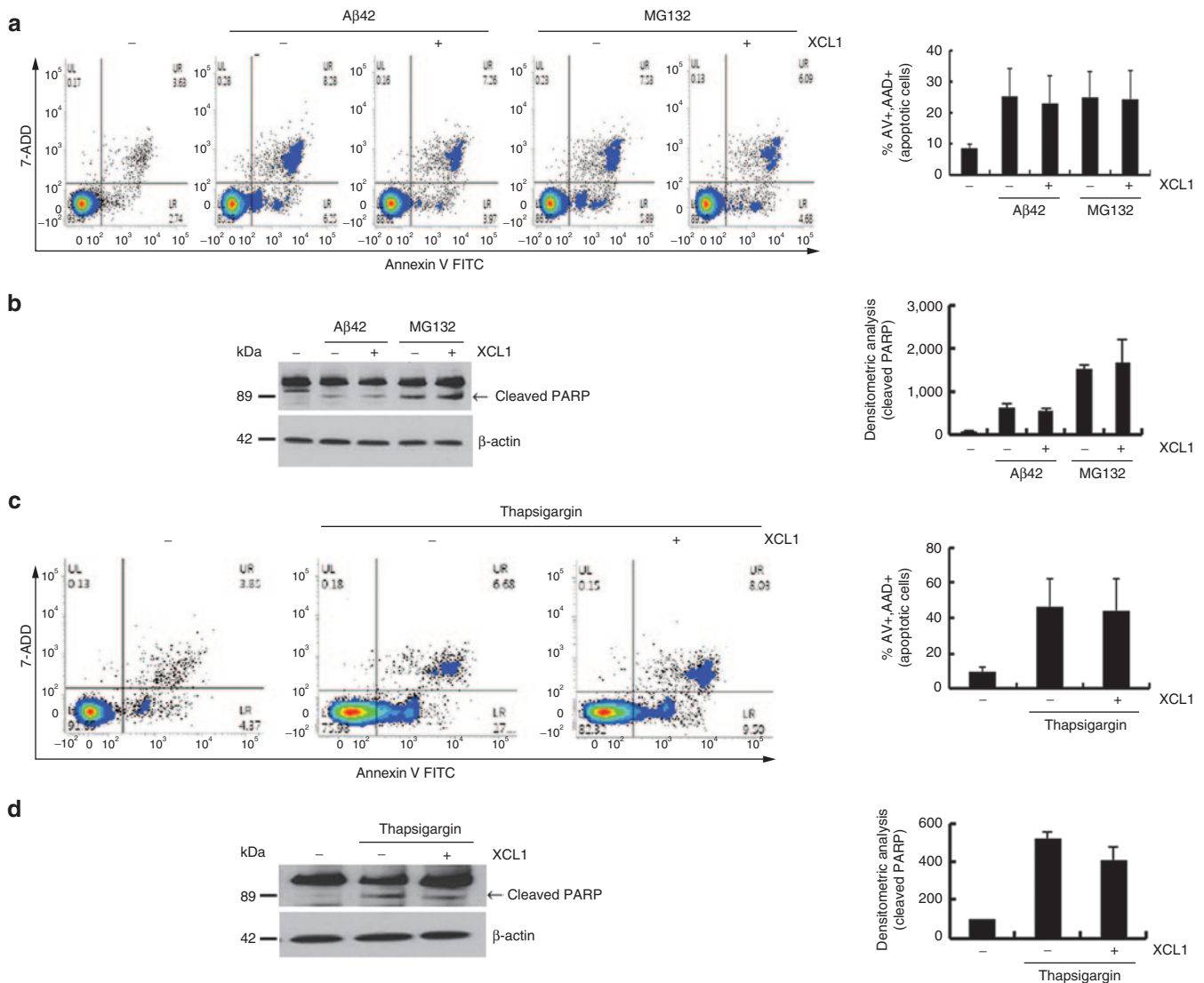


Figure 4 Absence of anti-apoptotic effect of XCL1 in other types of cells. The HT22, mouse hippocampal neuron cells were treated with amyloid-β42 (1 μmol/l for 48 hours) or MG132 (5 μmol/l for 24 hours) in the absence or presence of XCL1. **(a)** Fluorescence-activated cell-sorting (FACS) analysis of cells stained with annexin V/7-AAD. **(b)** Poly ADP-ribose polymerase (PARP)-cleaved bands were analyzed by densitometry. S16 rat Schwann cells were treated with thapsigargin (0.1 μmol/l for 12 hours) in the absence or presence of XCL1. The thapsigargin (0.1 μmol/l for 12 hours) treated S16 cells were analyzed by **(c)** FACS analysis and **(d)** Western blot analysis with anti-PARP antibody.

encoding a muscle isozyme of adenylosuccinate synthase, as a novel causative gene in distal myopathy and demonstrated its pathological roles in skeletal muscles.²⁸ In our previous study, zebrafish myopathy models were generated by knocking down the zebrafish *adssl1* gene using morpholino oligonucleotides (MOs). In this study, we tested whether the muscle defects shown in the *adssl1* MO-injected zebrafish embryos (morphants) were associated with muscle cell death, and then the human XCL1 was expected to encompass anti-apoptotic role in the skeletal muscles (Figure 7). Results of the TUNEL assay indicated that cell death in the trunk of *adssl1* morphants was higher than in the control morphants at 20 hours post fertilization (hpf), when both slow and fast muscle fibers are formed (Figure 7a). We further focused on the skeletal muscle cells and counted the dead cells within the area of five somites in each morphant. The data

showed higher death of muscle cells in the *adssl1* morphants, as compared to controls (Figure 7b–d). We introduced the human recombinant XCL1 protein into the *adssl1* morphants and examined cell death to determine if human XCL1 inhibits loss of *adssl1*-induced cell death in zebrafish. The results showed that the exogenous human XCL1 significantly reduced the death of skeletal muscle cells in the *adssl1* morphants (Figure 7a,c,d). The results of TUNEL assay 36 hpf when muscle progenitors are differentiated and functional were consistent with those of 20 hpf zebrafish embryos (Figure 7e–h). Furthermore, the number of dead cells counted in the brain of *adssl1* morphants and human XCL1-introduced *adssl1* morphants were not significantly different from those of control (Supplementary Figure S4). These *in vivo* data supported that XCL1 plays a negative role in skeletal muscle-specific apoptosis caused by *adssl1* depletion.

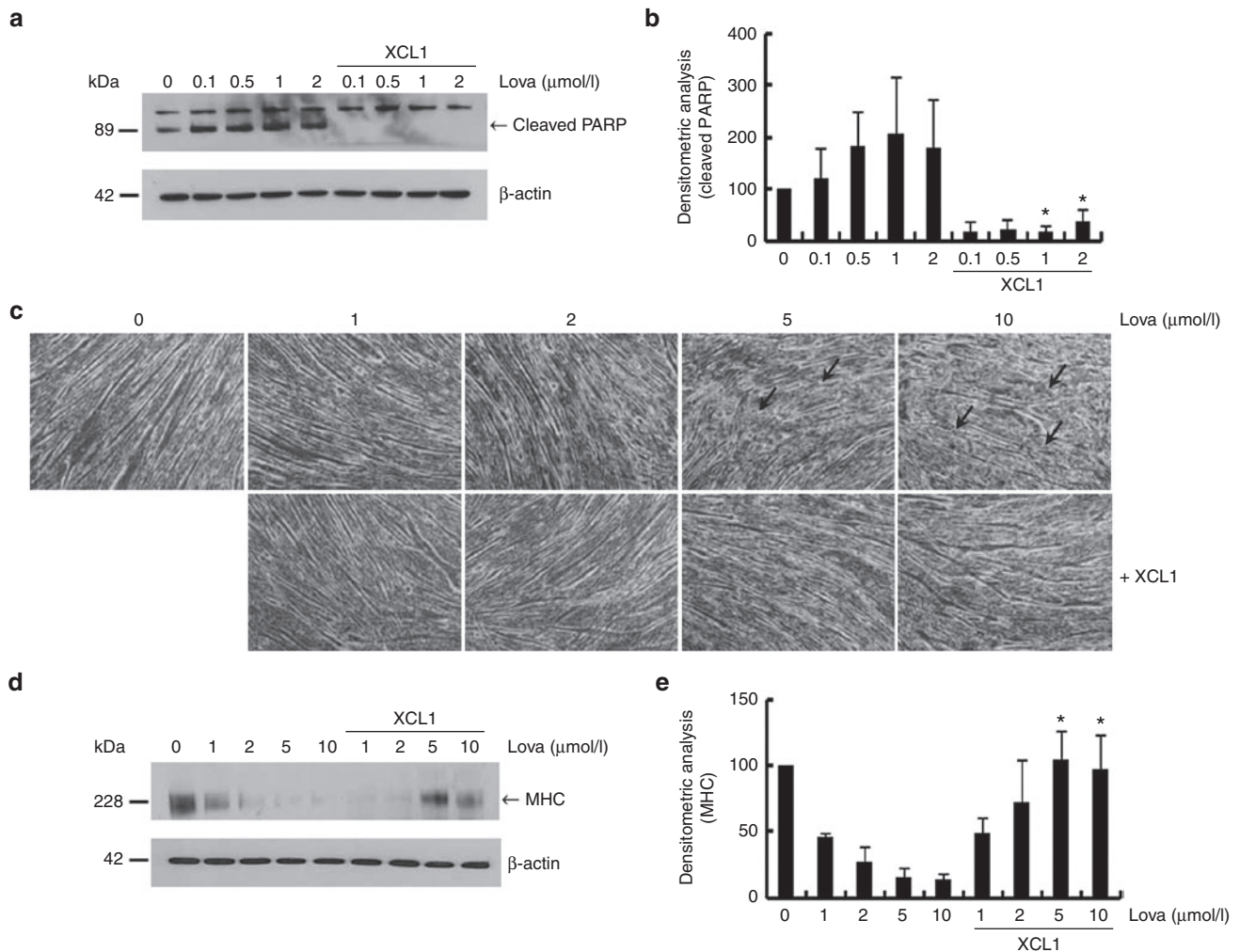


Figure 5 XCL1 treatment inhibited lovastatin-induced apoptosis of C2C12 cells and reduction of myotube formation. **(a)** C2C12 cells were treated with lovastatin (0.1, 0.5, 1, and 2 μmol/l) in a dose-dependent manner in the absence or presence of XCL1 and protein lysates were analyzed by Western blot analysis using anti-poly ADP-ribose polymerase (PARP) antibody. **(b)** Cleaved PARP fragments were monitored by densitometric analysis ($*P < 0.05$, $n = 3$). **(c)** The 7-day differentiated myotubes from C2C12 cells were treated with lovastatin (1, 2.5, 5, and 10 μmol/l) in the absence or presence of XCL1. Each arrow indicates defects in the myotubes. **(d,e)** Protein extracts of myotubes were analyzed by Western blot analysis using anti-myosin heavy chain (MHC) antibody. Bands of MHC were monitored by densitometric analysis ($*P < 0.05$, $n = 3$).

Human XCL1 rescues muscular dystrophy phenotypes in zebrafish

Based on our data as well as from previous reports suggesting possible roles of chemokines in regeneration of damaged muscles,²⁹ the therapeutic effect of human XCL1 was examined on the defective muscles in zebrafish. Gross morphological defects including curved body shape in *adssl1* morphants were largely restored by expression of human XCL1 in a dose-dependent manner (**Supplementary Figure S5**). Furthermore, we examined recovery of disrupted muscle tissues in human XCL1-expressed *adssl1* morphants. We evaluated skeletal muscles in specific areas of zebrafish trunk at 36 hpf (**Figure 8a**). We compared myoseptas, marked with anti-Laminin antibody, and myofibers, marked with anti-myosin heavy chain antibody in the skeletal muscles between phosphate-buffered saline (PBS)- and human XCL1-injected *adssl1* morphants. The results demonstrated recovery of irregular and gapped myofibers and U-shaped myoseptas in *adssl1* morphants to an extent similar to control embryos by dose-dependent expression of human XCL1

(**Figure 8b**). The zebrafish embryos with restored skeletal muscles were counted and the quantified data revealed rescue of over 30% of *adssl1* morphants by 50 μg/ml of human XCL1 (**Figure 8c; Supplementary Table S1**). Overall, our results suggested that anti-apoptotic role of XCL1 is pivotal not only for skeletal muscle development but also for regeneration of damaged muscles.

DISCUSSION

Recently, the importance of human MSCs protein secretion in the field of stem cell and regenerative medicine has been emphasized as many of these proteins mediate therapeutic effects in many disease models.^{30–32} Therefore, key secretory proteins of human MSCs are also used directly as novel treatments for patients and could be potent biomarkers for selection of superior human MSCs during large-scale cultivation of clinical grade human MSC in Good Manufacturing Practice facilities.³³ Based on these findings, we aimed to determine if either human MSCs or a selection of key secreted proteins may be applicable as novel treatments.

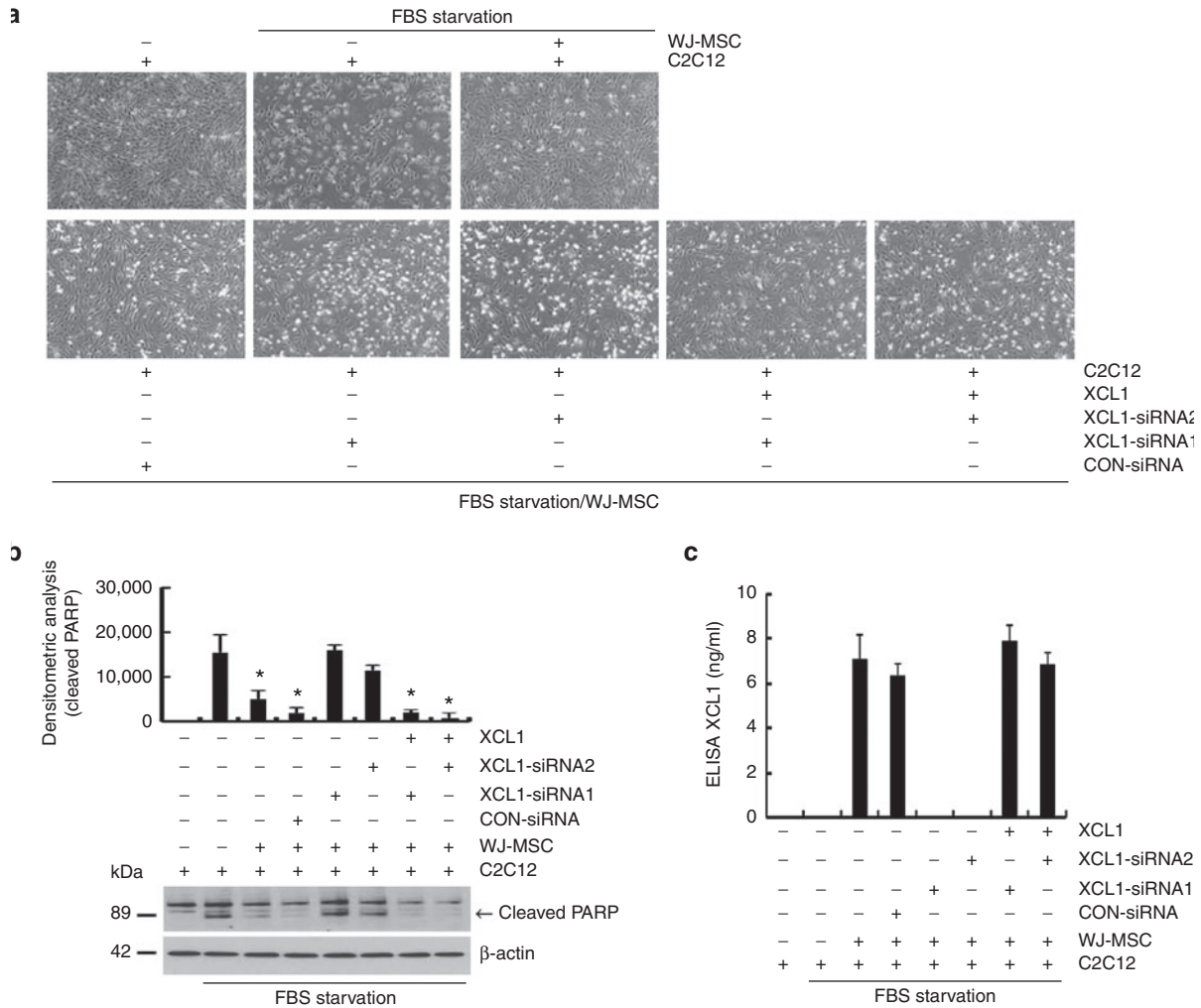


Figure 6 XCL1 siRNA treatment abolished anti-apoptotic effect of human Wharton’s jelly-derived human mesenchymal stem cell (WJ-MSC). **(a)** Before coculturing with serum-starved C2C12 cells, WJ-MSCs were separately pretreated with two siRNAs of human XCL1 containing different sequences for 24 hours. Each siRNA-treated WJ-MSC was cocultured with serum-deprived C2C12 cells for 12 hours. Human-recombinant XCL1 was added to cocultured C2C12 cells with siRNA-treated WJ-MSC to monitor gain of function of XCL1. C2C12 cell images were taken at each condition. **(b)** Cell lysates were analyzed by Western blot using anti-poly ADP-ribose polymerase (PARP) antibody. Cleaved PARP fragments were monitored by densitometric analysis ($*P < 0.05$, $n = 3$). **(c)** Secreted XCL1 concentration in each conditioned media was measured by XCL1 ELISA kit ($*P < 0.05$, $n = 3$).

There are many proposed causes of muscle disorders, such as genetic mutation, damage by exercise, aging, mitochondrial defect, and inflammation⁶⁻⁸ and in all the cases, myoblast death or abnormality of myotubes appears to as the final form of muscle disease.^{34,35} Therefore, protection from either muscle cell death or reduction of myotubes may be effective treatment strategy for muscle disorders, in particular, through the development of novel stem cell therapies using human MSCs. In Duchenne muscular dystrophy, it has been hypothesized that MSC treatment may facilitate muscle cell repair via anti-inflammatory effects and production of soluble factors to stimulate production of endogenous stem cells in muscles.³⁶⁻³⁸ Although several research groups have proposed various mechanisms for exertion of therapeutic effects of human MSC on some skeletal muscle diseases, any specific molecular mechanisms of human MSC protein secretion is not yet fully understood.

In this study, we established whether human WJ-MSCs have therapeutic effects on myoblast death and reduction of myotube formation using mouse skeletal myoblast C2C12 cells and *in vivo*

Zebrafish model of muscle disease. When C2C12 cells or C2C12 differentiated myotubes were exposed to cellular stresses such as serum deprivation or Lovastatin, both the cells showed typical patterns of cell death including PARP cleavage. When damaged C2C12 cells and myotubes were cocultured separately with WJ-MSCs in a transwell chamber, events like protection from cell death and loss of myotube were observed. XCL1 was identified as an active secretory protein from WJ-MSCs based on analyses of the shared medium of two different cell types grown in a transwell chamber without any cell contact. Highly elevated levels of XCL1 as a chemokine in the medium of WJ-MSCs cocultured with serum-starved C2C12 cells were noted, as compared to WJ-MSC alone. In order to determine that XCL1 is the critical factor for mediating anti-apoptotic effects of WJ-MSC, skeletal muscle cells or myotubes were treated with recombinant XCL1 protein under conditions of stress such as serum starvation and presence of Lovastatin. Treatment with recombinant XCL1 dramatically protected the cells from serum deprivation-induced C2C12 cell

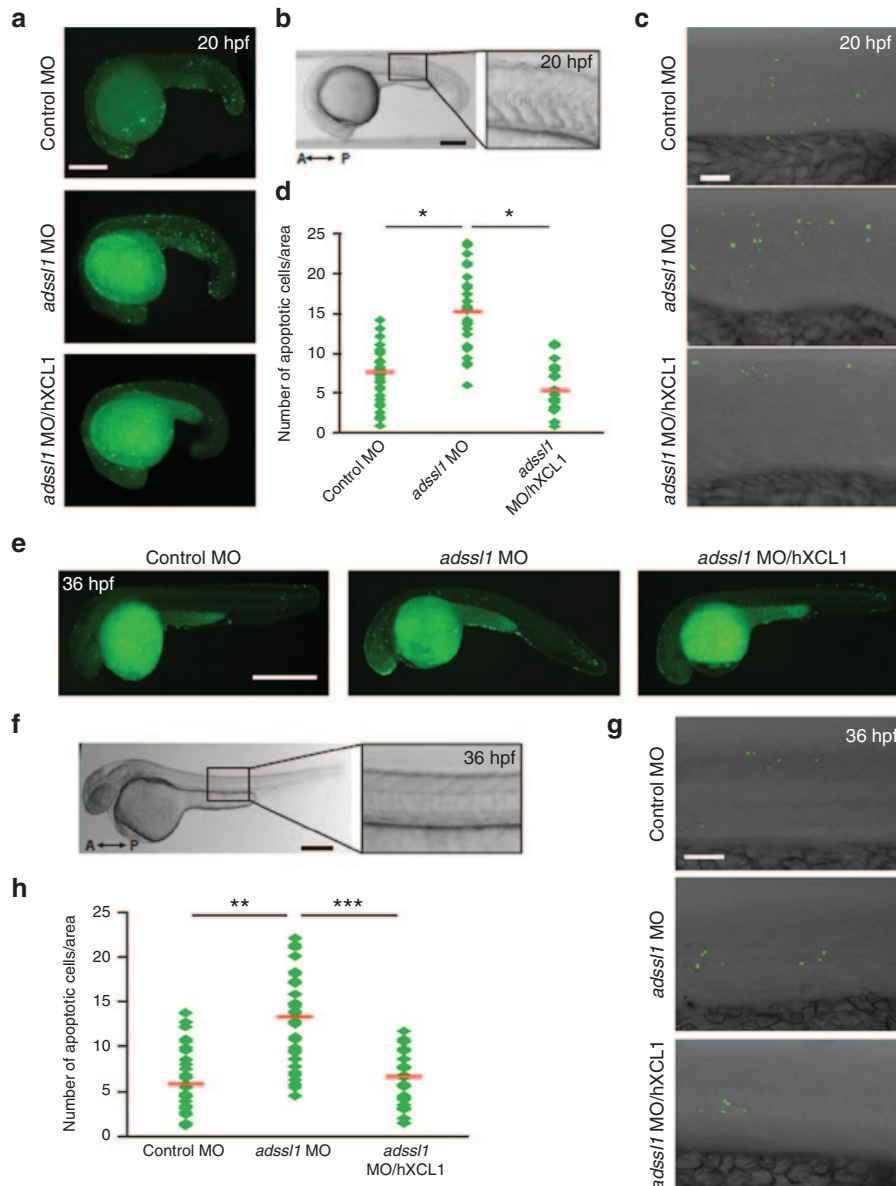


Figure 7 Induction of human XCL1 reduces apoptosis of the skeletal muscles in the zebrafish myopathy model. Twenty hours post fertilization (hpf) zebrafish embryos (**a–d**) and 36 hpf embryos were observed (**e–h**). (**a,e**) The apoptotic cells of control and *adssl1* morphants or human XCL1-induced *adssl1* morphants were detected by TUNEL assay, and the whole-mounted embryos were observed by fluorescent microscopy. (**b,f**) The boxed region of the embryos was photographed using confocal microscopy. (**c,g**) The representative confocal images show that the number of dead cells in *adssl1* morphants was more than in control morphants, and induction of human XCL1 inhibited the increase of cell death in *adssl1* morphants. (**d,h**) The cell death in the selected area (within five somites in the trunk) was quantified and presented in the scattered chart. A, anterior; P, posterior. **a,e**, bar = 100 μ m; **b,c,f,g**, bar = 50 μ m. **d,h**, Student's *t*-test: * $P < 0.05$, ** $P < 0.005$, *** $P < 0.001$.

apoptosis and reduction of differentiated myotubes. Conversely, pretreatment of WJ-MSC with siRNA for XCL1 abolished these effects in serum-starved C2C12 cells. Furthermore, XCL1 was found to inhibit apoptosis of skeletal muscle cells and anti-apoptotic function was found to be important to restore damaged muscles as well as for muscle development in an *in vivo* study conducted using the zebrafish model system.

To the best of our knowledge, ours is the first report to demonstrate anti-apoptotic property of human WJ-MSC-derived XCL1 in both *in vitro* and *in vivo* models of skeletal muscle disease. Chemokine (C motif) ligand (XCL1) is a small cytokine belonging to the XC chemokine family that is also known as lymphotactin.

High levels of XCL1 are reported in the spleen, thymus, intestines, and peripheral blood leukocytes, and lower levels in the lungs, prostate gland, and ovaries. Cellular sources for XCL1, which attracts T cells by binding to a chemokine receptor called XCR1, include activated thymic and peripheral blood CD8+ T cells.^{39,40} The anti-apoptotic role of XCL1 has not been reported even in the well-known immune system.

Recently, we identified a novel myopathy causative gene encoding ADSSL1 from distal myopathy individuals and succeed in generation of zebrafish myopathy model by knocking down of *adssl1* gene.²⁸ In our results, *in vivo* zebrafish myopathy models generated by *adssl1* targeting MOs injection showed typical

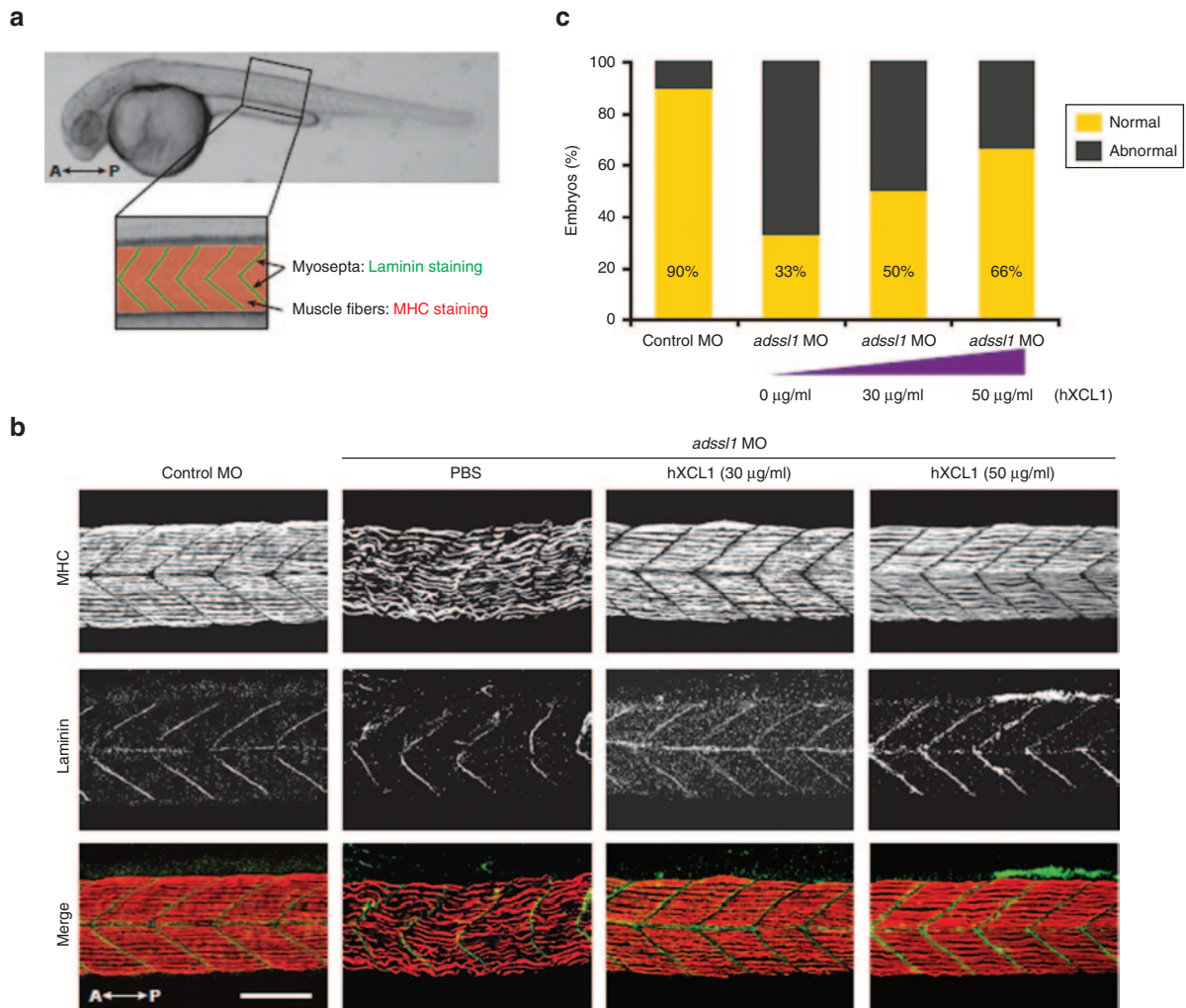


Figure 8 The rescue of defective skeletal muscles by human XCL1 in the zebrafish model. **(a)** The boxed region indicates the observed area to determine the effect of human XCL1 on skeletal muscles in zebrafish at 36 hpf. Myosepta and muscle fibers were stained with anti-Laminin and myosin heavy chain (MHC) antibodies, respectively. **(b)** The whole-mounted embryos after double staining with anti-Laminin and MHC antibodies were observed by confocal microscopy. The *adssl1* morphants (phosphate-buffered saline injected embryos) showed disrupted muscle fibers and myosepta, whereas the morphants injected with human XCL1 showed recovery of muscle defects. **(c)** The zebrafish embryos demonstrating skeletal muscle phenotype were counted and quantified data were presented graphically. The data indicates that human XCL1 restores muscle abnormality of *adssl1* morphants in a dose-dependent manner. A, anterior; P, posterior. Scale bar = 50 µm.

cell death patterns accompanied by positive TUNEL staining. However, after injecting human XCL1 protein in *adssl1* zebrafish myopathy models, TUNEL staining-positive cells were dramatically reduced. The effects of XCL1 are likely to be skeletal muscle cell favorable, since recombinant XCL1 treatment failed to prevent toxic amyloid-β42 or MG132-mediated apoptosis of HT22 mouse neurons and thapsigargin-induced S16 rat Schwann cell death. Moreover, in *in vivo* zebrafish myopathy models, the number of dead cells in the brain of *adssl1* morphants and human XCL1-introduced *adssl1* morphants were not significantly different from those of control and *adssl1* morphants.

The most notable anti-apoptotic factor of MSC is stanniocalcin-1 (STC-1), which is a multifunctional protein reducing apoptosis of lung cancer epithelial cells, induced by incubation at low pH in hypoxia or reactive oxygen species generation.⁴¹ Moreover, it has been reported that MSCs can promote A549 lung cancer cell survival by regulating mitochondrial respiration via STC-1.⁴²

Interestingly, this research group tested the anti-apoptotic effects of recombinant STC-1 in rat models of inherited retinal degeneration models through intravitreal injection.⁴² In another important study, the authors clearly proved intravitreal recombinant STC-1 as a promising therapy for retinal degeneration models.⁴³

Typical apoptotic patterns such as morphological changes, DNA fragmentation, and expression of apoptotic proteins have been observed in patient biopsies from dystrophinopathies, atrophy, myopathies with mitochondria dysfunction or inflammation, and exercise-induced muscle damage.^{6–10} Therefore, it is hypothesized that inhibition of apoptosis could be a novel treatment strategy for skeletal muscle disorders.^{11,35,44} In addition, human MSCs that exert anti-apoptotic, inflammatory, and immunomodulatory effects on the surrounding cells by the secretion of paracrine factors have been suggested as an effective therapeutic agent for muscle diseases. Accordingly, our findings that demonstrate human WJ-MSC and WJ-MSC-derived XCL1 play negative role in apoptosis of skeletal

muscle cells suggest a possible application of the recombinant XCL1 protein as a novel treatment of skeletal muscle diseases

MATERIALS AND METHODS

Cell culture. This study was approved by the Institutional Review Board of Samsung Medical Center, and informed consent was obtained from pregnant mothers. MSCs were isolated and expanded from WJ as described previously with some modifications.^{45,46} Human umbilical cords were kindly provided by Prof. Jong-Hwa Kim at Samsung Medical Center, Republic of Korea. The umbilical cord was washed several times with PBS and cut into 3–4 cm long pieces. After removal of blood vessels and amnion, tissues were minced into pieces using scissors. The minced tissues were incubated with 2 mg/ml of collagenase (Gibco BRL, Grand Island, NY) for 60–90 minutes and further digested with 0.25% trypsin (Gibco BRL, Grand Island, NY) for 30 minutes under gentle agitation at 37 °C. After addition of fetal bovine serum (Gibco BRL), the digested mixture was centrifuged at 1,000g for 10 minutes at room temperature (RT). Finally, the resulting mixture was washed with serum-free Dulbecco's Modified Eagle's medium and the cells (1,000–3,000 cells/cm²) were cultured in Dulbecco's Modified Eagle's medium supplemented with 20% fetal bovine serum and 1% penicillin-streptomycin (Gibco BRL) in a humidified incubator in 5% CO₂ at 37 °C. In our study, the minimal yield of WJ-MSCs from 20 donated umbilical cords was found to be >50%. We used all WJ-MSCs at passage 6. The C2C12, a mouse myoblast cell line, (ATCC CRL-1772, American Type Culture Collection, Rockville, MD) was cultured in Dulbecco's Modified Eagle's medium (Biowest S.A.S, Nuaille, France) supplemented with 20% fetal bovine serum (Gibco BRL), 100 U/ml penicillin, and 100 µg/ml streptomycin (Gibco) in 5% CO₂ at 37 °C. When C2C12 cells reached 80–90% confluency, apoptosis was induced through serum starvation for 12 and 24 hours, respectively. For coculture experiments with C2C12 cells, WJ-MSCs (1.5 × 10⁵ cells) were seeded into transwell chambers (pore size 1 µm, BD Biosciences, Franklin Lakes, NJ) at indicated times. The C2C12 myoblasts (1 × 10⁵ cells/well of a six-well plate) were treated with or without human recombinant XCL1 (0–5 nmol/l) (R&D Systems, Minneapolis, MN) for indicated time periods in serum-free medium. When C2C12 cells reached 80–90% confluency, the culture medium was replaced with a differentiation medium supplemented with 2% horse serum (Gibco BRL) for induction of myotube formation. Subsequent to 6–7 days of inducing differentiation, cells were used for further experiments.⁴⁷ C2C12 cells and differentiated myotubes were treated with varying concentrations of lovastatin as (0.1, 0.5, 1, 2 µmol/l) or (1, 2.5, 5, 10 µmol/l), respectively, to promote cell death with subsequent treatment with or without various concentrations of XCL1 (0–5 nmol/l) for 24 hours in a serum-free state.

siRNA treatment. For knock down of XCL1 expression, control siRNA or XCL1 targeting siRNAs (Bioneer, Republic of Korea) were mixed with Lipofectamine 2000 reagent (Invitrogen, Carlsbad, CA). WJ-MSCs were treated with the mixture for 24 hours in a serum-free medium. Control siRNA with at least four mismatches to any human, mouse, or rat gene was used.

Flow cytometry. Cell suspensions were stained using FITC Annexin V Apoptosis Detection Kit with 7-AAD (Bio Legend, San Diego, CA) according to the manufacturer's instructions. The cells (70–80%) were resuspended in 500 µl 1× staining buffer. Subsequently, 5 µl Annexin V and 5 µl 7-AAD were slowly added to the binding buffer for 20–30 minutes at RT in dark, prior to being analyzed by flow cytometry (BD Biosciences, Franklin Lakes, NJ). Data regarding percentages of Annexin V-positive apoptotic and 7-AAD-positive necrotic cells are shown. Cytotoxicity results included data about Annexin V-positive and/or 7-AAD-positive cells.

Western blot analysis. Cell extracts were prepared by ultra-sonication (Branson Ultrasonics, Danbury, CT) using a buffer containing 9.8 mol/l urea, 4% CHAPS, 130 mmol/l dithiothreitol, 40 mmol/l Tris-HCl, 0.1% sodium dodecyl sulfate, 1 mmol/l ethylenediaminetetraacetate, and a protease/phosphatase inhibitor cocktail. Protein quantification was performed using the Bradford assay (Bio-rad Laboratories, Hercules, CA). Protein extracts

(20 µg) were separated by SDS-PAGE and the resolved proteins were transferred to nitrocellulose membranes. Each membrane was incubated with the above mentioned antibodies. The membranes were blocked with 5% skim milk in TBS-T (containing 0.2% Tween-20) at RT with gentle shaking for 60 minutes, followed by incubation with primary antibodies (1:1,000 dilution in 5% skim milk) for 1–1.5 hours at RT or overnight (4 °C) with gentle shaking. After washing in TBS-T (3×, 10 minutes/wash), membranes were incubated with horseradish peroxidase-conjugated anti-rabbit or mouse secondary antibodies (1:5,000 in 5% skim milk) at RT for 1 hour with gentle shaking. The membranes were washed (3×, 10 minutes/wash) and treated with the ECL solution (Advansta, Republic of Korea) for 3 minutes before detecting the bands through film exposure.

Antibody arrays. Secreted proteins in the media collected from the experiments were measured using the RayBio Biotin Label-based Human Antibody Array (#AAH-BLG-1–4), according to recommended protocols. The array can detect 507 human proteins. All slides were scanned using the Axon's GenePix 4000B scanner and analyzed using GenePix Pro 6.0. The average score of the triplicates was normalized using internal controls.

Zebrafish husbandry. Zebrafish were raised and maintained by following standard protocols. The procedure included maintain them at 28.5 °C with 13 hours light 10 hours dark cycle in a recirculating tank system using local tap water (pH 7.5–7.9, Genomic Design Bioengineering Company, Korea). Adult wild-type AB strains were bred to obtain embryos. Developmental stages of the embryos were determined using morphological features of fish at each observed time point.

Microinjection of morpholino and protein. Microinjection was performed using PV830 Pneumatic PicoPump (World Precision Instruments). For generating the zebrafish myopathy model, anti-sense MOs were obtained from Gene Tools. The standard control MO (5'-CCTCTTACCTCAGTTACAATTTATA-3') and *adssl1* splicing-blocking MO (5'-ATAAAGGGTGTGGTCCCTACATTGA-3') targeting the intron 9 and exon 9 of *adssl1* were dissolved in distilled water and microinjected into 1–2 cell stage embryos at a concentration of 4 ng per embryo. Recombinant Human XCL1/Lymphotactin protein (R&D Systems) was injected into 12 hpf embryos at concentration level of 30 or 50 µg/ml each. Embryos were incubated at 28.5 °C in 1× E3 media (5.0 mmol/l NaCl, 0.17 mmol/l KCl, 0.43 mmol/l CaCl₂, 0.4 mmol/l MgCl₂, pH 7.2) and 0.2 mmol/l 1-phenyl-2-thiourea (Sigma, St. Louis, MO) was added to inhibit melanin formation.

Whole-mount immunostaining of zebrafish. For whole-mount immunostaining, 36 hpf embryos were dechorionated and fixed in 4% paraformaldehyde for 1 hour at RT. After two washes with PBS, embryos were blocked with blocking solution (2% bovine serum albumin, 0.5% Triton X-100, 0.05% dimethyl sulfoxide (DMSO), and 5% normal goat serum in 1× PBS) for 2 hours at RT. Anti-laminin antibody (1:50, Sigma, L9393) and anti-myosin antibody (1:50, Developmental Studies Hybridoma Bank, Boston, F59) were diluted in blocking solution and incubated at 4 °C overnight. After washing with PBST (0.5% TritonX-100 in 1× PBS), embryos were incubated at RT for 2 hours with Alexa Flour-594-conjugated anti-mouse secondary antibody and Alexa Flour-488-conjugated anti-rabbit secondary antibody (1:200, Invitrogen, A11005) in 2% NGS/PBST. Embryos were washed with PBST four times and mounted in 70% glycerol/PBS. Analysis of zebrafish muscle was conducted using confocal microscope (Zeiss LSM700), and the images were processed and analyzed using Zeiss ZEN imaging software (Zeiss, Germany).

Detection of cell death in zebrafish. Apoptotic cells in zebrafish were examined by TUNEL assay. Dechorionated embryos were fixed with 4% paraformaldehyde overnight at 4 °C and washed with PBS twice. Fixed embryos were dehydrated with 100% methanol overnight at –20 °C and gradually rehydrated with 75%, 50%, and 25% methanol for 15 minutes at RT. The embryos were permeabilized with 0.1% sodium citrate in PBST (0.1% TritonX-100 in 1× PBS). After washing in PBST, embryos were incubated with labeling solution and enzyme solution (In Situ Cell Death Detection

Kit, Fluorescein; Roche, Nutley, NJ) for 3 hours at 37 °C in a dark room. Images were captured by mono-camera (DS-Qi2; Nikon, Tokyo, Japan) and analyzed using the NIS-Elements software (Nikon, Tokyo, Japan) to detect and analyze the apoptotic cells.

Antibodies and reagents. The following primary antibodies were used for the experiment: PARP (Cell Signalling Technology, Danvers, MA), Myosin Heavy Chain (R&D Systems), and β -actin (Santa Cruz Biotechnology, Santa Cruz, CA). As reagent vehicle, Lovastatin (>98% purity, mevino-lin; Sigma-Aldrich) was prepared as a 25 mmol/l stock solution in DMSO (Sigma-Aldrich) and the PAN Caspase Inhibitor (Z-V-A-D(OMe)-FMK) (R&D Systems) was prepared as a 50 mmol/l stock solution in DMSO. These reagents were further diluted in DMSO prior to cell treatment. Human XCL1/Lymphotactin (R&D Systems) was prepared as a 100 μ g/ml stock solution in Dulbecco's phosphate-buffered saline.

Statistical analyses. Data are presented as means \pm SE. The statistical comparison between the groups was performed by a *t*-test. Differences were considered statistically significant when the calculated *P* value was <0.05. The Excel 2010 software for windows was used for all analyses.

SUPPLEMENTARY MATERIAL

Figure S1. Images of serum-starved C2C12 cells taken at 12 and 24 hours in the absence or presence of WJ-MSC.

Figure S2. Characterization of human WJ-MSC.

Figure S3. Anti-apoptotic effect of XCL1 is not observed in other types of cells.

Figure S4. No effect of human XCL1 on apoptosis in non-skeletal muscle regions of zebrafish.

Figure S5. The effect of human XCL1 on developmental morphology of zebrafish *adssl1* morphants.

Table S1. The number of zebrafish embryos showing normal/abnormal skeletal muscles after double staining with anti-Laminin and MHC antibodies.

ACKNOWLEDGMENTS

This study was supported by a grant from the Basic Research Program through the National Research Foundation of South Korea (NRF) grant funded by the Korean government (MSIP) (2014R1A2A1A11050576 to J.W.C. and 2013R1A1A1059056 to J.E.L.). Korean Health Technology R&D Project, Ministry of Health and Welfare, Republic of Korea (H114C3484). The authors declare no conflict of interest.

REFERENCES

- Daniel, NN and Korsmeyer, SJ (2004). Cell death: critical control points. *Cell* **116**: 205–219.
- Portt, L, Norman, G, Clapp, C, Greenwood, M and Greenwood, MT (2011). Anti-apoptosis and cell survival: a review. *Biochim Biophys Acta* **1813**: 238–259.
- Li, J and Yuan, J (2008). Caspases in apoptosis and beyond. *Oncogene* **27**: 6194–6206.
- Taylor, RC, Cullen, SP and Martin, SJ (2008). Apoptosis: controlled demolition at the cellular level. *Nat Rev Mol Cell Biol* **9**: 231–241.
- Adhithy, PJ and Hood, DA (2003). Mechanisms of apoptosis in skeletal muscle. *Basic Appl Myol* **13**: 171–179.
- Sandri, M and Carraro, U (1999). Apoptosis of skeletal muscles during development and disease. *Int J Biochem Cell Biol* **31**: 1373–1390.
- Schwartz, LM (2008). Atrophy and programmed cell death of skeletal muscle. *Cell Death Differ* **15**: 1163–1169.
- Sandri, M, Rossini, K, Podhorska-Okolow, M and Carraro, U (1999). Role of Apoptosis in muscle disorders. *Basic Appl Myol* **9**: 301–310.
- Kumar, S and Harvey, NL (1995). Role of multiple cellular proteases in the execution of programmed cell death. *FEBS Lett* **375**: 169–173.
- McGeehan, GM, Becherer, JD, Bast, RC Jr, Boyer, CM, Champion, B, Connolly, KM et al. (1994). Regulation of tumour necrosis factor- α processing by a metalloproteinase inhibitor. *Nature* **370**: 558–561.
- Girgenrath, M, Dominov, JA, Kostek, CA and Miller, JB (2004). Inhibition of apoptosis improves outcome in a model of congenital muscular dystrophy. *J Clin Invest* **114**: 1635–1639.
- Testi, R (1996). Sphingomyelin breakdown and cell fate. *Trends Biochem Sci* **21**: 468–471.
- Hauvstetter, A and Izumo, S (1998). Apoptosis: basic mechanisms and implications for cardiovascular disease. *Circ Res* **82**: 1111–1129.
- Squillaro, T, Peluso, G and Galderisi, U (2016). Clinical trials with mesenchymal stem cells: an update. *Cell Transplant* **25**: 829–848.
- Kim, HJ, Seo, SW, Chang, JW, Lee, JI, Kim, CH, Chin, J et al. (2015). Stereotactic brain injection of human umbilical cord blood mesenchymal stem cells in patients with Alzheimer's disease dementia: a phase 1 clinical trial. *Alzheimers Dement* **1**: 95–102.
- Chang, YS, Ahn, SY, Yoo, HS, Sung, SI, Choi, SJ, Oh, WI et al. (2014). Mesenchymal stem cells for bronchopulmonary dysplasia: phase 1 dose-escalation clinical trial. *J Pediatr* **164**: 966–972.e6.
- Kim, DH, Lee, D, Chang, EH, Kim, JH, Hwang, JW, Kim, JY et al. (2015). GDF-15 secreted from human umbilical cord blood mesenchymal stem cells delivered through the cerebrospinal fluid promotes hippocampal neurogenesis and synaptic activity in an Alzheimer's disease model. *Stem Cells Dev* **24**: 2378–2390.
- Kim, JY, Kim, DH, Kim, JH, Lee, D, Jeon, HB, Kwon, SJ et al. (2012). Soluble intracellular adhesion molecule-1 secreted by human umbilical cord blood-derived mesenchymal stem cell reduces amyloid- β plaques. *Cell Death Differ* **19**: 680–691.
- Kim, JY, Kim, DH, Kim, DS, Kim, JH, Jeong, SY, Jeon, HB et al. (2010). Galectin-3 secreted by human umbilical cord blood-derived mesenchymal stem cells reduces amyloid- β neurotoxicity *in vitro*. *FEBS Lett* **584**: 3601–3608.
- Lee, RH, Pulin, AA, Seo, MJ, Kota, DJ, Ylostalo, J, Larson, BL et al. (2009). Intravenous hMSCs improve myocardial infarction in mice because cells embolized in lung are activated to secrete the anti-inflammatory protein TSG-6. *Cell Stem Cell* **5**: 54–63.
- Lee, RH, Yoon, N, Reneau, JC and Prockop, DJ (2012). Preactivation of human MSCs with TNF- α enhances tumor-suppressive activity. *Cell Stem Cell* **11**: 825–835.
- Caplan, AI and Correa, D (2011). The MSC: an injury drugstore. *Cell Stem Cell* **9**: 11–15.
- Caplan, AI and Harii, R (2015). Body management: mesenchymal stem cells control the internal regenerator. *Stem Cells Transl Med* **4**: 695–701.
- Kern, S, Eichler, H, Stoeve, J, Klüter, H and Bieback, K (2006). Comparative analysis of mesenchymal stem cells from bone marrow, umbilical cord blood, or adipose tissue. *Stem Cells* **24**: 1294–1301.
- Kadowaki, H, Nishitoh, H, Urano, F, Sadamitsu, C, Matsuzawa, A, Takeda, K et al. (2005). Amyloid beta induces neuronal cell death through ROS-mediated ASK1 activation. *Cell Death Differ* **12**: 19–24.
- Nishitoh, H, Matsuzawa, A, Tobiume, K, Saegusa, K, Takeda, K, Inoue, K et al. (2002). ASK1 is essential for endoplasmic reticulum stress-induced neuronal cell death triggered by expanded polyglutamine repeats. *Genes Dev* **16**: 1345–1355.
- Kislinger, T, Gramolini, AO, Pan, Y, Rahman, K, MacLennan, DH and Emili, A (2005). Proteome dynamics during C2C12 myoblast differentiation. *Mol Cell Proteomics* **4**: 887–901.
- Park, HJ, Hong, YB, Choi, YC, Lee, J, Kim, EJ, Lee, JS et al. (2016). ADSSL1 mutation relevant to autosomal recessive adolescent onset distal myopathy. *Ann Neurol* **79**: 231–243.
- McLennan, IS (1996). Degenerating and regenerating skeletal muscles contain several subpopulations of macrophages with distinct spatial and temporal distributions. *J Anat* **188** (Pt 1): 17–28.
- Baraniak, PR and McDevitt, TC (2010). Stem cell paracrine actions and tissue regeneration. *Regen Med* **5**: 121–143.
- Gnecchi, M, Zhang, Z, Ni, A and Dzau, VJ (2008). Paracrine mechanisms in adult stem cell signaling and therapy. *Circ Res* **103**: 1204–1219.
- Mirotsov, M, Zhang, Z, Deb, A, Zhang, L, Gnecchi, M, Noisieux, N et al. (2007). Secreted frizzled related protein 2 (Sfrp2) is the key Akt-mesenchymal stem cell-released paracrine factor mediating myocardial survival and repair. *Proc Natl Acad Sci USA* **104**: 1643–1648.
- Kolkundkar, U (2014). Cell therapy manufacturing and quality control: current process and regulatory challenges. *J Stem Cell Res Ther* **260**: 75–82.
- Liu, CC and Ahearn, JM (2001). Apoptosis of skeletal muscle cells and the pathogenesis of myositis: a perspective. *Curr Rheumatol Rep* **3**: 325–333.
- Stratos, I, Li, Z, Rotter, R, Herlyn, P, Mittlmeier, T and Vollmar, B (2012). Inhibition of caspase mediated apoptosis restores muscle function after crush injury in rat skeletal muscle. *Apoptosis* **17**: 269–277.
- Ichim, TE, Alexandrescu, DT, Solano, F, Lara, F, Campion, Rde N, Paris, E et al. (2010). Mesenchymal stem cells as anti-inflammatories: implications for treatment of Duchenne muscular dystrophy. *Cell Immunol* **260**: 75–82.
- Quattrocchi, M, Cassano, M, Crippa, S, Perini, I and Sampaolesi, M (2010). Cell therapy strategies and improvements for muscular dystrophy. *Cell Death Differ* **17**: 1222–1229.
- Sienkiewicz, D, Kulak, W, Okurowska-Zawada, B, Paszko-Patej, G and Kawnik, K (2015). Duchenne muscular dystrophy: current cell therapies. *Ther Adv Neurol Disord* **8**: 166–177.
- Kennedy, J, Kelner, GS, Kleyenstuber, S, Schall, TJ, Weiss, MC, Yssel, H et al. (1995). Molecular cloning and functional characterization of human lymphotactin. *J Immunol* **155**: 203–209.
- Yoshida, T, Imai, T, Takagi, S, Nishimura, M, Ishikawa, I, Yaoi, T et al. (1996). Structure and expression of two highly related genes encoding SCM-1/human lymphotactin. *FEBS Lett* **395**: 82–88.
- Block, GJ, Ohkouchi, S, Fung, F, Frenkel, J, Gregory, C, Pochampally, R et al. (2009). Multipotent stromal cells are activated to reduce apoptosis in part by upregulation and secretion of stanniocalcin-1. *Stem Cells* **27**: 670–681.
- Ohkouchi, S, Block, GJ, Katsha, AM, Kanehira, M, Ebina, M, Kikuchi, T et al. (2012). Mesenchymal stromal cells protect cancer cells from ROS-induced apoptosis and enhance the Warburg effect by secreting STC1. *Mol Ther* **20**: 417–423.
- Roddy, GV, Rosa, RH Jr, Oh, JY, Ylostalo, JH, Bartosh, TJ Jr, Choi, H et al. (2012). Stanniocalcin-1 rescued photoreceptor degeneration in two rat models of inherited retinal degeneration. *Mol Ther* **20**: 788–797.
- Meinen, S, Lin, S, Thurnherr, R, Erb, M, Meier, T and Rügge, MA (2011). Apoptosis inhibitors and mini-agrin have additive benefits in congenital muscular dystrophy mice. *EMBO Mol Med* **3**: 465–479.
- Mitchell, KE, Weiss, ML, Mitchell, BM, Martin, P, Davis, D, Morales, L et al. (2003). Matrix cells from Wharton's jelly form neurons and glia. *Stem Cells* **21**: 50–60.
- Peng, J, Wang, Y, Zhang, L, Zhao, B, Zhao, Z, Chen, J et al. (2011). Human umbilical cord Wharton's jelly-derived mesenchymal stem cells differentiate into a Schwann-cell phenotype and promote neurite outgrowth *in vitro*. *Brain Res Bull* **84**: 235–243.
- Sultan, KR, Henkel, B, Terlou, M and Haagsman, HP (2006). Quantification of hormone-induced atrophy of large myotubes from C2C12 and L6 cells: atrophy-inducible and atrophy-resistant C2C12 myotubes. *Am J Physiol Cell Physiol* **290**: C650–C659.